NEURAL REGENERATION RESEARCH
December 2016, Volume 11, Issue 12
www.nrronline.org

RESEARCH ARTICLE

Biodegradable magnesium wire promotes regeneration of compressed sciatic nerves

Bo-han Li[1, 2] **Ke Yang**[3], **Xiao Wang**[4, *]

1 Department of Oral & Maxillofacial Surgery, The General Hospital of the People's Liberation Army, Beijing, China
2 Department of Oral & Maxillofacial Surgery, Binzhou Medical University, Yantai, Shandong Province, China
3 Metal Research Institute of Chinese Academy of Sciences, Shenyang, Liaoning Province, China
4 Department of Oral & Maxillofacial Surgery, Peking University Third Hospital, Beijing, China

How to cite this article: *Li BH, Yang K, Wang X (2016) Biodegradable magnesium wire promotes regeneration of compressed sciatic nerves. Neural Regen Res 11(12):2012-2017.*

Funding: *This work was supported by the National Natural Science Foundation of China, No. 81400528; the China Postdoctoral Science Foundation, No. 20130390827.*

Graphical Abstract

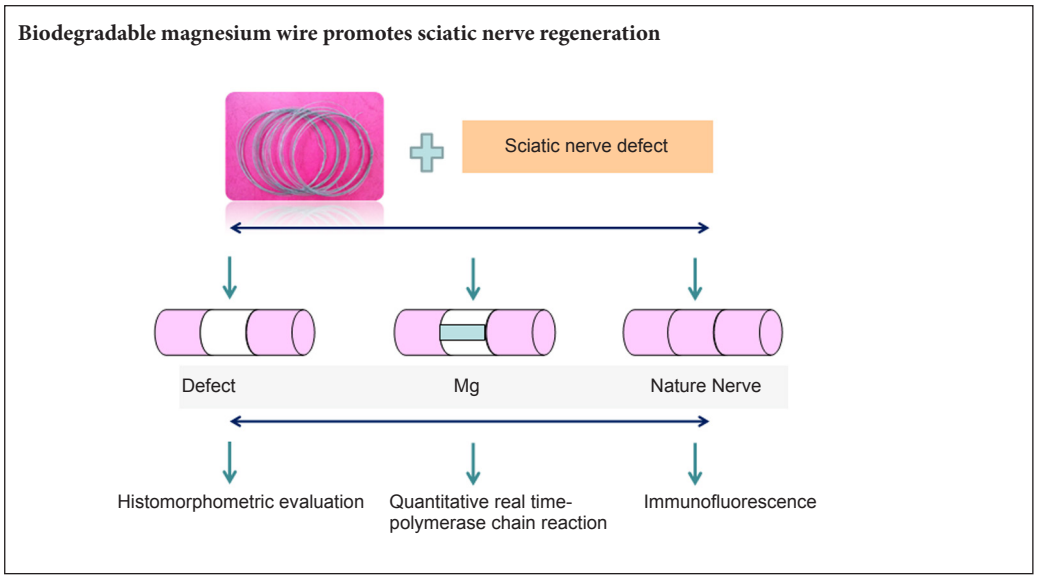

***Correspondence to:**
Xiao Wang,
bysywangxiao@163.com.

orcid:
0000-0003-3710-026X
(Xiao Wang)

doi: *10.4103/1673-5374.197146*

Accepted: *2016-11-12*

Abstract

Magnesium (Mg) wire has been shown to be biodegradable and have anti-inflammatory properties. It can induce Schwann cells to secrete nerve growth factor and promote the regeneration of nerve axons after central nervous system injury. We hypothesized that biodegradable Mg wire may enhance compressed peripheral nerve regeneration. A rat acute sciatic nerve compression model was made, and AZ31 Mg wire (3 mm diameter; 8 mm length) bridged at both ends of the nerve. Our results demonstrate that sciatic functional index, nerve growth factor, p75 neurotrophin receptor, and tyrosine receptor kinase A mRNA expression are increased by Mg wire in Mg model. The numbers of cross section nerve fibers and regenerating axons were also increased. Sciatic nerve function was improved and the myelinated axon number was increased in injured sciatic nerve following Mg treatment. Immunofluorescence histopathology showed that there were increased vigorous axonal regeneration and myelin sheath coverage in injured sciatic nerve after Mg treatment. Our findings confirm that biodegradable Mg wire can promote the regeneration of acute compressed sciatic nerves.

Key Words: *nerve regeneration; peripheral nerve regeneration; biodegradable; magnesium wire; sciatic nerve; rats; nerve growth factor; P75 neurotrophin receptor; tyrosine receptor kinase A; neural regeneration*

Introduction

Peripheral nerve injury results in total or partial sensory, motor, and trophic action loss. Peripheral nerve injury commonly occurs as a result of diseases, tumors, and traumatic injury. The prevalence of peripheral nerve lesions varies between 2% and 2.8%, increasing to 5% if plexus and radicular nerve lesions are included (Eser et al., 2009; Buchaim et al., 2015). Many studies have investigated the enhancement or acceleration of injured peripheral nerve recovery, with inconsistent results (Li et al., 2012, 2015; He et al., 2016).

A variety of biological tissues, natural and synthetic polymers have been adapted for use as nerve conduits. Biodegradable polymers, such as polylactic acid, polyglycolic acid, polylactic-co-glycolic acid, and polycaprolactone, enable nerve regeneration, showing comparable results to autografts (Jang et al., 2016). In addition to their advantageous flexibility, degradable magnesium (Mg) alloys provide an ideal degradation time and strength. Vennemeye et al. (2015) used Mg filaments (0.25 mm diameter, 10 mm length) covered with biodegradable nerve conduits to repair 6 mm gap injuries in sciatic nerves. Mg supplementation of the diet can enhance crushed sciatic nerve regeneration (Pan et al., 2011). Mg wire has better flexibility and a smoother surface than other metallic material, which is suitable for Schwann cell adhesion. It can also be totally absorbed within 2 weeks (Li, 2013). Given these considerations, we constructed a biodegradable Mg wire made of AZ31 Mg and applied it to a sciatic nerve crush injury model. Our aim was to evaluate whether biodegradable magnesium wire has effects on sciatic nerve regeneration.

Materials and Methods

Animals

Thirty-six male Sprague-Dawley rats, aged 6 weeks and weighing approximately 200–250 g, were purchased from an animal supplier (KeYu Co., China) (SCXK (Jing) 2016-0002). The experiments were performed 1 week after housing adaptation. All procedures were carried out in accordance with the Care Guidelines of the Laboratory Animal Care and Use Committees of First Affiliated Hospital of PLA General Hospital, China.

The rats were equally and randomly divided into three groups: injury group (acute compression injury of sciatic nerve), injury + Mg group, and sham group.

Establishment of sciatic nerve injury model and insertion of biodegradable Mg wire

The rats were intraperitoneally anesthetized using sodium pentobarbital (40 mg/kg) and the right sciatic nerve exposed through a gluteal muscle splitting approach. In the injury group, an 8-mm long silastic tube (1 mm internal diameter; 2 mm outer diameter; Shanghai Daoguan Rubber Products Factory, Shanghai, China) was cut longitudinally, and atraumatically wrapped around the sciatic nerve. The longitudinal split in the tube was then closed tightly using 8-0 sutures (Shanghai Pudong Jinhuan Medical Product Co., Ltd., Shanghai, China) for 3 hours. In the injury + Mg group, the same procedure was conducted and part of the epineurium was cut distal to the defect. A biodegradable Mg-3%Al-1%Zn (AZ31) wire (diameter 3 mm) (supported by Metal Research Institute of Chinese Academy of Sciences) was then put through the sciatic nerve epineurium (**Figure 1**). In the sham group, the right sciatic nerves were exposed, and then sutured, without silastic placement.

Sciatic functional index (SFI)

Four weeks after surgery, SFI was assessed in six rats from each group according to a previous study (Reynolds and Weiss, 1992). The rats walked through a 1 m long tunnel with white paper on the floor and ink on their hind feet. The footprints of normal feet (N) and experimental feet (E) were marked and evaluated with three parameters: the length of the footprint from third toe to heel (PL); the width of toes from first toe to the fifth toe (TS); and the width of middle toes from the second toe to the fourth toe (ITS). SFI was calculated according to the formula described by Varejao et al. (2004): SFI = −38.3 [(EPL − NPL)/NPL] + 109.5 [(ETS − NTS)/NTS] + 13.3 [(EITS − NITS)/NITS] − 8.8. SFI values range from 0 for normal nerve function, to around −100 for complete nerve dysfunction (Zeng et al., 2013; Buchaim et al., 2015).

Histomorphometric evaluation

At the end of the 4-week follow-up, the sciatic nerves from six rats were exposed again, and the nerve segments, including the injury site, were harvested. The nerves were immediately immersed into a fixation solution of 2.5% glutaraldehyde in phosphate buffered saline (PBS) (pH 7.4) at 4°C for 24 hours.

Only the distal portion (5 mm distal to the injury site) was used for histomorphometric evaluation. The nerve segment was postfixed in 2% osmium tetroxide for 2 hours, washed with PBS (pH 7.4), routinely processed and embedded in epoxy resin. Serial transverse sections (1 μm thick) were cut using an ultramicrotome (Ultracut, Leica, Milano, Italy) and stained with 1% toluidine blue for light microscopy

Table 1 Primer sequences

Gene	Sequence (5′–3′)	mRNA position (start)	mRNA position (end)	Product size (bp)
NGF	Forward: AAG ACC ACA GCC ACG GAC AT Reverse: CGC CTT GAC AAA GGT GTG AG	722	916	195
$p75^{NTR}$	Forward: TGG CGG ATA TGG TGA CCA CT Reverse: GCA GCT GTT CCA CCT CTT GA	770	921	152
TrkA	Forward: AGC CGT GGA ACA GCA TCA CT Reverse: CGC ATG GTC TCA TTG GTC AG	943	1095	153
GAPDH	Forward: GCA TCC TGC ACC AAC T Reverse: GCA GTG ATG GCA TGG ACT GT	802	902	101

NGF: Nerve growth factor; $p75^{NTR}$: p75 neurotrophin receptor; TrkA: tyrosine receptor kinase A; GAPDH: glyceraldehyde-3-phosphate dehydrogenase.

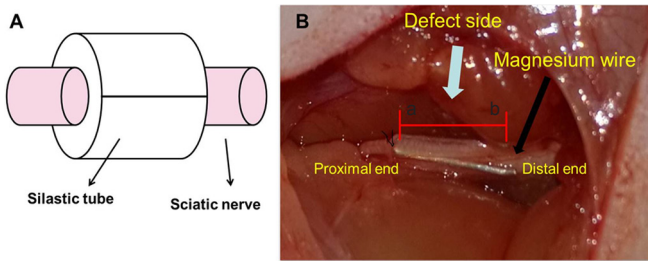

Figure 1 Sciatic nerve defect bridged by biodegradable magnesium wire.
(A) Sciatic nerve defect: acute sciatic nerve compression was performed using an 8-mm long silastic tube (1 mm internal diameter; 2 mm outer diameter) for 3 hours. (B) The sciatic nerve defect side (white arrow) was bridged by magnesium wires (black arrow); a: the proximal end; b: the distal end.

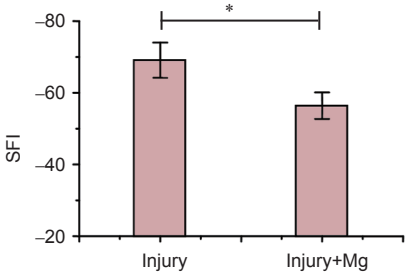

Figure 2 Sciatic functional index (SFI) in rats 4 weeks after surgery.
SFI was lower in the injury group than in the injury + Mg group, *P < 0.05. Data are expressed as the mean ± SEM (n = 12, Mann-Whitney U test). Mg: Magnesium.

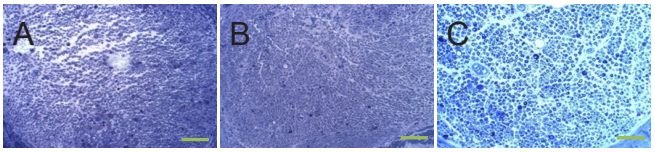

Figure 3 Histological features in semithin sections distal to the crush injury site at 4 weeks postoperatively (toluidine blue staining, × 400).
(A) Injury group (acute compression defect of sciatic nerve): dystrophic appearance and incompact axon. (B) Injury + Mg group: typical regenerating nerves tending to cluster in minifascicles. (C) Sham group: right sciatic nerves were only exposed, without silastic placement. Scale bar: 100 μm. Mg: Magnesium.

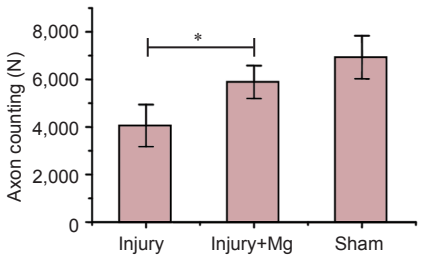

Figure 4 Axon counting on the injury side of each group.
The number of myelinated axons was larger in the injury + Mg group than in the injury group (*P < 0.05), but lower than in the sham group. All data are presented as the mean ± SEM (n = 6, one-way analysis of variance followed by *post hoc* least significant difference test). Injury group: acute compression defect of sciatic nerve; injury + Mg group: acute compression defect of sciatic nerve and placement of Mg (AZ31) wires; sham group: the right sciatic nerves were only exposed, without silastic placement. Mg: Magnesium.

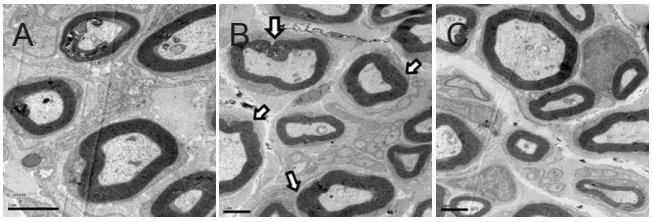

Figure 5 Transmission electron microscopy of transverse sections of sciatic nerves 4 weeks after surgery.
(A) Injury group: acute compression defect of sciatic nerve. (B) Injury + Mg group: acute compression defect of sciatic nerve and placement of Mg (AZ31) wires; regenerated myelinic (white arrows) nerve fibers. (C) Sham group: the right sciatic nerves were only exposed, without silastic placement. Uranyl acetate and lead citrate double staining, × 4,000; transmission electron microscope. Scale bars: 2 μm. Mg: Magnesium.

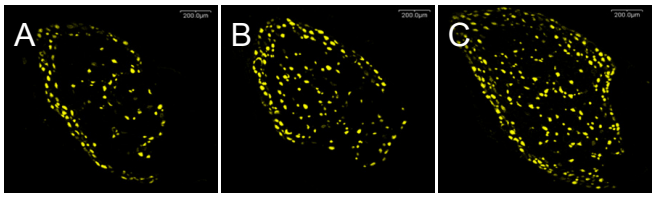

Figure 7 Retrograde labeling of dorsal root ganglion neurons with Fluoro-Gold at 4 weeks after surgery (confocal microscopy, × 200).
(A) Sham group: the right sciatic nerves were only exposed, without silastic placement. (B) Injury group: acute compression defect of sciatic nerve. (C) Injury + Mg group: acute compression defect of sciatic nerve and placement of Mg wires. More Fluoro-Gold-labeled neurons were visible in the injury + Mg group than in the injury group.

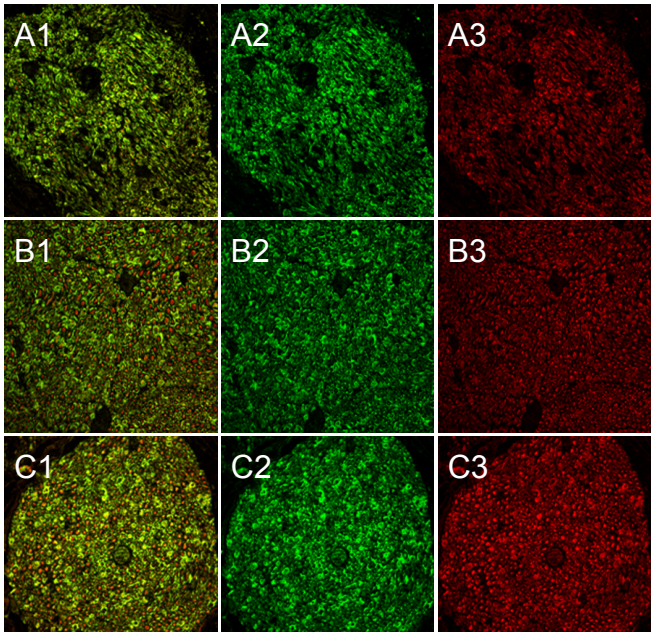

Figure 8 The distal nerve stump 4 weeks after surgery (red NF200, green S100; × 200; confocal microscopy).
(A1–A3) Injury group (acute compression defect of sciatic nerve); (B1–B3) injury + Mg group (acute compression defect of sciatic nerve and placement of Mg wires); (C1–C3) sham group (the right sciatic nerves were exposed, without silastic placement). More vigorous axonal regeneration and myelin sheath (NF200 and S100 positive) coverage was observed in the injury + Mg group than in the injury group. NF200: Neurofilament 200.

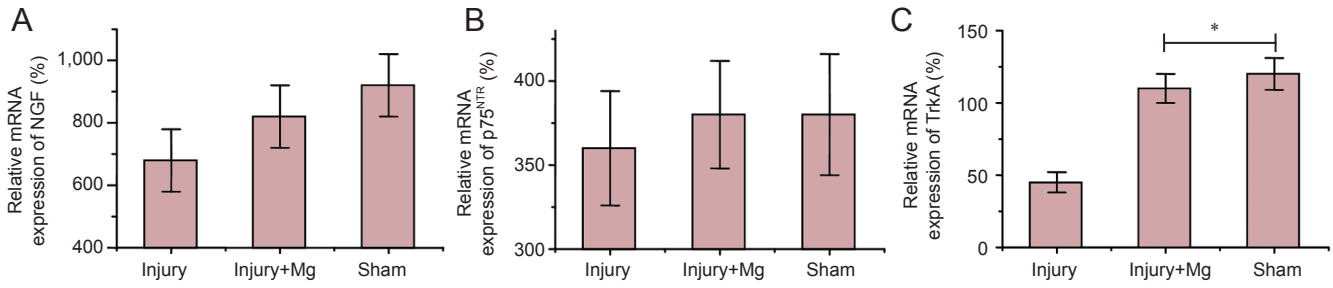

Figure 6 Quantification (relative expression, %) of NGF, p75^{NTR}, and TrkA mRNA expression in the sciatic nerve at 4 weeks after operation by quantitative real time-polymerase chain reaction.

NGF (A) and p75^{NTR} (B) mRNA expression levels were higher in the injury + Mg group than in the injury group. (C) TrkA mRNA expression level was significantly higher in the injury + Mg group than in the injury group (*P = 0.041). All data are presented as the mean ± SEM (n = 6; one-way analysis of variance followed by *post hoc* least significant difference test). Experiments were conducted at least twice. Injury group: acute compression defect of sciatic nerve; injury + Mg group: acute compression defect of sciatic nerve and placement of Mg (AZ31) wires; sham group: the right sciatic nerves were only exposed, without silastic placement.

(Olympus, BX41, TF, Japan). Images were captured using a specialized SPOT RT-KE color mosaic system (Diagnostic Instruments Inc., Sterling Heights, MI, USA) and digitized by SPOT Ver. 4.6 software (Diagnostic Instruments Inc.). For myelinated axon counting, the total cross-sectional area of the nerve was first visualized at 40× magnification. Three fields were then randomly selected for observation at 200× magnification. Mean fiber density was calculated by dividing the total number of myelinated nerve fibers within the field by its area (n/mm^2). Total fiber number (n) was then estimated by multiplying the mean fiber density by the total area of the whole nerve cross section, assuming a uniform distribution of nerve fibers across the entire section (Chen et al., 2009; Li et al., 2012).

To observe axon and myelin sheath regeneration in more detail, ultrathin cross sections (60–70 nm) were cut using the ultramicrotome and double-stained with uranyl acetate and lead citrate. The sections were analyzed using a transmission electron microscope (JSM 1200 IIEX, JEOL, Tokyo, Japan)

Quantitative real time-polymerase chain reaction (RT-PCR) analyses

Dissociated L_4 and L_5 spinal cords from three rats of each group were prepared at 4 weeks after the surgical procedure. Total RNA was extracted from spinal cords using Trizol reagent (Invitrogen, Carlsbad, CA, USA). mRNA encoding NGF, p75 neurotrophin receptor (p75^{NTR}), and tyrosine receptor kinase A (TrkA) receptor were reverse transcribed to cDNA using a first-strand synthesis kit (Invitrogen). The amount of cDNA was also quantified using RT-PCR. Primers for the following transcripts were used to amplify specific cDNA regions of interest: NGF, p75^{NTR}, TrkA, and glyceraldehyde- 3-phosphate dehydrogenase (GAPDH) (GenBank reference sequences XM_227523.3, X05137.1, M85214.1, and NM_017008.3, respectively). The primer information is listed in **Table 1**. GAPDH quantification was used as an internal control for normalization. The PCR cycling conditions were: 95°C for 20 seconds, 40 cycles of 95°C for 20 seconds, and 59°C for 30 seconds. The percentage differences of mRNA levels over control values were calculated using the cycle threshold ($2^{-\Delta\Delta Ct}$) method as described previously (Applied Biosystems Manual, Foster City, CA, USA) according to references (Chen et al., 2009; Li et al., 2012). PCR reactions were repeated at least twice.

Retrograde labeling and quantification of dorsal root ganglion (DRG)

L_4 and L_5 DRG neurons were retrograde labeled with a fluorescent dye, Fluoro-Gold (Molecular Probes, Eugene, OR, USA) at 4 weeks postoperatively. After anesthesia, the crushed sciatic nerves were cut, and Fluoro-Gold was put on the distal side of the proximal part of the sciatic nerve and then sutured. After 5 days, the rats were deeply anesthetized and perfused with saline and paraformaldehyde as described previously (Savignat et al., 2008; Li et al., 2012). The ipsilateral L_4 and L_5 DRGs were removed and postfixed overnight with paraformaldehyde. DRGs were immersed in a 20% sucrose solution for 4 days, embedded in Tissue Tek (Sakura, Tokyo, Japan), and frozen in liquid nitrogen. Serial 35 μm longitudinal sections were cut at −20°C using a cryostat microtome (CM30505 Cryostat, Leica). Sections were then observed under a fluorescence microscope equipped with a rhodamine filter (Olympus FV-300). The number of Fluoro-Gold-positive neurons in each DRG was counted. The positive-labeled neurons at the DRG section of each group were randomly selected, and their area (soma size of neuron) was measured and averaged using computer software (OPTIMAS Ver. 6.5) (Savignat et al. 2008).

Immunofluorescence and histopathology

Four weeks after surgery, the sciatic nerves were removed, fixed in 4% paraformaldehyde for 12 hours, then put in 30% sucrose phosphate buffer for 24 hours until they sunk to the bottom of the container. A cryostat microtome was then used to cut 20–30 μm thick cross sections. The primary antibodies mouse anti-S100 (1:500; Sigma, St. Louis, MO, USA), and anti-neurofilament 200 (1:80; Sigma) were applied overnight at 4°C. Secondary antibodies goat anti-rabbit IgG (FITC) and goat anti-mouse IgG (TRITC) (both Sigma) were applied for 1 hour at room temperature

(He et al., 2016; Wang et al., 2016). Images were acquired using a laser confocal microscope (FV10i-oil, push around, Tokyo, Japan).

Statistical analysis

Data analysis was carried out by using StatView software (Version 5.0.1, SAS Institute, Cary, NC, USA) to reveal the mean ± SEM. One-way analysis of variance followed by *post hoc* least significant difference test was used to compare axon counting, as well as for quantitative RT-PCR results. The Mann-Whitney *U* test for SFI was used. A *P* value of 0.05 or less was considered statistically significant.

Results

SFI

SFI revealed different improvements in each group 4 weeks after operation. SFI was significantly higher in the injury + Mg group (–47.7 ± 2.5) than in the injury group (–59.4 ± 3.7) ($P < 0.05$; **Figure 2**).

Regenerated nerve morphology

Transverse nerve sections exhibited different typical appearances of regenerating nerves (**Figure 3A–C**). These were characterized by the presence of myelinated fibers of small and medium sizes, clustered in small fascicles with an enlarged area of connective matrix. The number of axons in the injury + Mg group was higher compared with the injury group. The number of regenerated myelinated nerve fibers was significantly higher in the injury + Mg group than in the injury group ($P = 0.041$; **Figure 4**).

The histological profiles of both groups were similar to mixed myelinated and unmyelinated fibers of variable diameters undergoing obvious regeneration within a Wallerian degeneration background. Transmission electron microscopy findings showed the presence of regenerated myelinic nerve fibers in the injury + Mg group (**Figure 5A–C**).

mRNA levels of NGF, $p75^{NTR}$, and trkA

Quantitative RT-PCR revealed that NGF, $p75^{NTR}$, and trkA mRNA levels were slightly lower in the injury + Mg group than in the sham group.TrkA mRNA expression was significantly higher in the injury + Mg group than in the injury group ($P = 0.041$; **Figure 6**).

Retrograde labeling (FG) after rat sciatic nerve repair with biodegradable magnesium wire

Representative photomicrographs of retrograde ganglion labeling are illustrated in **Figure 7**. The number of Fluoro-Gold-positive DRG neurons was greater in the injury + Mg group than in the injury group.

Immunofluorescence result after rat sciatic nerve repair with biodegradable magnesium wire

Four weeks after surgery, cross sections of the distal nerve stumps were observed after staining with neurofilament 200 and S100. Vigorous regenerating nerve fibers and myelin sheath were greater in the injury + Mg group than in the injury group (**Figure 8**).

Discussion

After peripheral nerve injury, the distal portions of axons separate from the trophic center (cell body) and degenerate in a series of steps called Wallerian degeneration (Jang et al., 2016). Successful treatments for traumatic defects of the peripheral nerve have been limited (Shahraki et al., 2015). A critical issue in peripheral nerve regeneration with an artificial nerve conduit is inducing sufficient Schwann cells from the bilateral severed nerve stump as the first steps toward nerve regeneration. In this study, we observed the morphology of regenerated nerves bridged by biodegradable Mg wire in the early period of nerve regeneration. During surgery, the biodegradable Mg wire was found to be easy to use and had good adhesive properties.

Immunohistochemistry revealed that the expression of special proteins in axons and myelin sheath was more evident in the injury + Mg group than in the sham group, which indicated a normal histological structure of regular circle shape. The location of S100 and NF200 in the injury + Mg group was more positive fluorescence signal than in the injury group. This further implies the presence of regenerated axons and Schwann cell-like cells, accompanied by the myelination and structural recovery of regenerated nerve fibers, similar to a previous report (Shahraki et al., 2015). Histomorphometric evaluations lead us to the same conclusion; the number of myelinated axons in the injury + Mg group was larger than in the injury group. The presence of blood vessels is important, as they facilitate the regeneration of nerves (Viterbo et al., 2009; Buchaim et al., 2015).

Our results reveal that recovery from peripheral nerve lesions is possible with the use of Mg wire. In our model, it was an effective method for assisting the recovery of compression defect nerves. The morphology of nerve fibers at different stages directly demonstrates the maturation of axons, which is also a marker for assessing the efficiency of indirect conduit bridging. Many of the fibers with small diameters could be nonconducting and degenerating rather than regenerating. As the nerve fibers regenerate distally and reach the appropriate target organs, the fiber diameter increases and the myelin sheath grows (Buchaim et al., 2015; Cheng et al., 2015; Golzadeh and Mohammadi, 2016).

The SFI values in this study show that after a compression injury in the sciatic nerve, there is a functional loss in both experimental groups at 4 weeks post-surgery. Statistical analysis revealed significant differences between the injury + Mg group and the injury group.

We choose 4 weeks as the observation period as Mg absorption occurs within 2 weeks. Once it has been absorbed we do not know what plays the most important role in regeneration of the compressed sciatic nerve, the Mg or natural nerve recovery processes.

Several reports have found that a high-Mg diet improves neurological functional recovery and enhances nerve regeneration in mice with sciatic nerve injuries. Pan et al. (2011) used a high-Mg diet (TestDiet containing 0.7 mg/g Mg and

supplemented by $MgCl_2$ 0.5 mg/mL in water) for 3 weeks before experiments and 4 weeks after sciatic nerve injury and found that Mg deficiency markedly enhanced the inflammatory response, while Mg supplementation counteracted the inflammatory response. Similar reports (Vennemeye et al., 2015) also suggest that biodegradable Mg metal filaments placed inside biodegradable nerve conduits might provide the physical guidance support needed to improve the rate and extent of regeneration of peripheral nerves across injury gaps.

We also found that Mg wire induced fibrosis. At 4 weeks after surgery, we harvested nerve tissue for histomorphometric evaluation and found fibrosis in the end where the Mg wire connected with the defective nerve. Li et al. (2016) also found the fibrosis in DRG in chronic sciatic nerve compression experiments.

A previous study showed that Mg implants at the beginning were probably due to the gas after the first rapid corrosion following the surgery. Despite the resorption of this plate/screw system, wound healing was not affected (Galli et al., 2015; Schaller et al., 2016). Due to the density and resolution ratio of X-ray between the gas and the nerve tissue, it is difficult to detect the bubble after putting Mg wire in the sciatic nerve.

Our preliminary data suggest that Mg wire can promote axonal regeneration after peripheral nerve injury. However, the underlying mechanism for nerve regeneration remains to be further elucidated. Although the current study did not clarify that Mg wire played the key role in such process, to our knowledge, this is the first experiment to show the role of Mg in peripheral nerve regeneration after injury in animal models. We conclude that biodegradable Mg wire can promote the regeneration of acute compressed sciatic nerves.

Acknowledgments: *We thank Metal Research Institute of Chinese Academy of Sciences in China for providing AZ31 Mg.*
Author contributions: *BHL was responsible for animal surgery, cell preparation and data processing. XW had full access to all data and participated in analysis of both data integrity and data accuracy. KY participated in the preparation of biodegradable magnesium wire. All authors approved the final version of the paper.*
Conflicts of interest: *None declared.*
Plagiarism check: *This paper was screened twice using CrossCheck to verify originality before publication.*
Peer review: *This paper was double-blinded and stringently reviewed by international expert reviewers.*

References

Buchaim RL, Andreo JC, Barraviera B, Ferreira Junior RS, Buchaim DV, Rosa Junior GM, de Oliveira AL, de Castro Rodrigues A (2015) Effect of low-level laser therapy (LLLT) on peripheral nerve regeneration using fibrin glue derived from snake venom. Injury 46:655-660.
Chen Y, Wang D, Wang Z, Weng Z, Deng Z (2009) Effect of adenovirus expressing NGF on sciatic nerve injury in rats. Zhongguo Xiufu Chongjian Waike Zazhi 23:947-953.
Cheng XL, Wang P, Sun B, Liu SB, Gao YF, He XZ, Yu CY (2015) The longitudinal epineural incision and complete nerve transection method for modeling sciatic nerve injury. Neural Regen Res 10:1663-1668.
Eser F, Aktekin LA, Bodur H, Atan C (2009) Etiological factors of traumatic peripheral nerve injuries. Neurology India 57:434-437.
Galli S, Naito Y, Karlsson J, He W, Andersson M, Wennerberg A, Jimbo R (2015) Osteoconductive potential of mesoporous titania implant surfaces loaded with 6.magnesium: an experimental study in the rabbit. Clin Implant Dent Relat Res 17:1048-1059.
Golzadeh A, Mohammadi R (2016) Effect of local administration of platelet-derived growth factor B on functional recovery of peripheral nerve regeneration: a sciatic nerve transection model. Dent Res J 13:225-232.
He X, Ao Q, Wei Y, Song J (2016) Transplantation of miRNA-34a overexpressing adipose-derived stem cell enhances rat nerve regeneration. Wound Repair Regen 24:542-550.
Jang CH, Lee H, Kim M, Kim G (2016) Effect of polycaprolactone/collagen/hUCS microfiber nerve conduit on facial nerve regeneration. Int J Biol Macromol 12:1-8.
Li BH, Liu HC (2012) Effect of Schwann cells proliferation on co-culture with magnesium. Zhongguo Laonianxue Zazhi 11:132-135.
Li BH, Kim SM, Yoo SB, Kim MJ, Jahng JW, Lee JH (2012) Recombinant human nerve growth factor (rhNGF-beta) gene transfer promotes regeneration of crush-injured mental nerve in rats. Oral Surg Oral Med Oral Pathol Oral Radiol 113:e26-34.
Li HF, Wang YR, Huo HP, Wang YX, Tang J (2015) Neuroprotective effects of ultrasound-guided nerve growth factor injections after sciatic nerve injury. Neural Regen Res 10:1846-1855.
Li Q, Chen J, Chen Y, Cong X, Chen Z (2016) Chronic sciatic nerve compression induces fibrosis in dorsal root ganglia. Mol Med Rep 13:2393-2400.
Pan HC, Sheu ML, Su HL, Chen YJ, Chen CJ, Yang DY, Chiu WT, Cheng FC (2011) Magnesium supplement promotes sciatic nerve regeneration and down-regulates inflammatory response. Magnes Res 24:54-70.
Reynolds BA, Weiss S (1992) Generation of neurons and astrocytes from isolated cells of the adult mammalian central nervous system. Science 255:1707-1710.
Savignat M, Vodouhe C, Ackermann A, Haikel Y, Lavalle P, Libersa P (2008) Evaluation of early nerve regeneration using a polymeric membrane functionalized with nerve growth factor (NGF) after a crush lesion of the rat mental nerve. J Oral Maxillofac Surg 66:711-717.
Schaller B, Saulacic N, Imwinkelried T, Beck S, Liu EW, Gralla J, Nakahara K, Hofstetter W, Iizuka T (2016) In vivo degradation of magnesium plate/screw osteosynthesis implant systems: soft and hard tissue response in a calvarial model in miniature pigs. J Craniomaxillofac Surg 44:309-317.
Shahraki M, Mohammadi R, Najafpour A (2015) Influence of tacrolimus (FK506) on nerve regeneration using allografts: a rat sciatic nerve model. J Oral Maxillofac Surg 73:e1431-1439.
Varejao AS, Melo-Pinto P, Meek MF, Filipe VM, Bulas-Cruz J (2004) Methods for the experimental functional assessment of rat sciatic nerve regeneration. Neurol Res 26:186-194.
Vennemeyer JJ, Hopkins T, Hershcovitch M, Little KD, Hagen MC, Minteer D, Hom DB, Marra K, Pixley SK (2015) Initial observations on using magnesium metal in peripheral nerve repair. J Biomater Appl 29:1145-1154.
Viterbo F, Amr AH, Stipp EJ, Reis FJ (2009) End-to-side neurorrhaphy: past, present, and future. Plast Reconstr Surg 124:e351-358.
Wang J, Muheremu A, Zhang M, Gong K, Huang C, Ji Y, Wei Y, Ao Q (2016) MicroRNA-338 and microRNA-21 co-transfection for the treatment of rat sciatic nerve injury. Neurol Sci 37:883-890.
Zeng X, Zhang L, Sun L, Zhang D, Zhao H, Jia J, Wang W (2013) Recovery from rat sciatic nerve injury in vivo through the use of differentiated MDSCs in vitro. Exp Ther Med 5:193-196.

Copyedited by Brooks W, Maxwell R, Wang J, Li CH, Qiu Y, Song LP, Zhao M